Journal of the Korean Magnetic Resonance Society **2017**, *21,* 90-95
DOI 10.6564/JKMRS.2017.21.3.090

NMR Study on the Preferential Binding of the Zα Domain of Human ADAR1 to CG-repeat DNA Duplex

Ae-Ree Lee, Seo-Ree Choi, Yeo-Jin Seo, and Joon-Hwa Lee*

Department of Chemistry and RINS, Gyeongsang National University, Jinju, Gyeongnam 52828, South Korea

Received Jul 24, 2017; Revised Jul 30, 2017; Accepted Aug 5, 2017

Abstract The Z-DNA domain of human ADAR1 ($Z\alpha_{ADAR1}$) produces B-Z junction DNA through preferential binding to the CG-repeat segment and destabilizing the neighboring AT-rich region.[9] However, this study could not answer the question of how many base-pairs in AT-rich region are destabilized by binding of $Z\alpha_{ADAR1}$. Thus, we have performed NMR experiments of $Z\alpha_{ADAR1}$ to the longer DNA duplex containing an 8-base-paired (8-bp) CG-repeat segment and a 12-bp AT-rich region. This study revealed that $Z\alpha_{ADAR1}$ preferentially binds to the CG-repeat segment rather than AT-rich region in a long DNA and then destabilizes at least 6 base-pairs in the neighboring AT-rich region for efficient B-Z transition of the CG-repeat segment.

Keywords NMR, Z-DNA binding protein, Z-DNA, B-Z junction DNA, DNA-protein complex

Introduction

Left-handed Z-form helix is a higher energy conformation of DNA than right-handed B-DNA.[1,2] Z-DNA could be formed under high salt condition, negative supercoiling and complex formation with Z-DNA binding proteins (ZBPs).[1-3] The crystal structures of various ZBPs in complex with 6-base-paired (6-bp) CG-repeat DNA found that the interaction with Z-DNA is mediated by the α3 helix and in the β-hairpin.[4-7]

When the ZBPs produce Z-DNA segments in a genomic DNA, two B–Z junctions at each end of Z-DNA should be formed. A crystal structural study of the Zα domain of human ADAR1 ($Z\alpha_{ADAR1}$) complexed with 15-bp DNA showed that DNA are stabilized at one end in the Z-conformation by $Z\alpha_{ADAR1}$ proteins, while the other end remains B-DNA.[8] Recently, NMR studies have suggested a three-step mechanism of B–Z junction formation: (*i*) binding of $Z\alpha_{ADAR1}$ to the CG-rich DNA segment maintaining B-DNA, (*ii*) B-Z conversion of the CG-rich segment, and (*iii*) formation of the B–Z junction structure.[9,10] The hydrogen exchange studies revealed that the short AT-rich region was greatly destabilized like a bulge structure upon binding of $Z\alpha_{ADAR1}$ to the neighboring CG-repeat segment.[9,10]

During B–Z junction formation of DNA, the question of how many base-pairs in AT-rich part are destabilized by specific binding of $Z\alpha_{ADAR1}$ to the CG-repeat segment still remains. Unfortunately, the previous NMR studies could not answer this question, because these studies were performed using 13-bp DNA duplexes which have only 5-bp AT-rich region (region II of bzDNA13 in Fig. 1).

To investigate more clearly the B–Z junction formation in a long DNA induced by $Z\alpha_{ADAR1}$, we have performed NMR titration experiments of $Z\alpha_{ADAR1}$ to a 20-bp DNA duplex which contains an

* Correspondence to: **Joon-Hwa Lee,** Department of Chemistry and RINS, Gyeongsang National University, Jinju, Gyeongnam 52828, Korea, Tel: 82-55-772-1490; E-mail: joonhwa@gnu.ac.kr

8-bp CG-repeat segment (denoted as BBZ-20, Fig. 1). The results provided the direct evidence that $Z\alpha_{ADAR1}$ prefers to bind to CG-repeat segments and then destabilizes the neighboring AT-rich part for B–Z transition. This study provides valuable insights into the molecular mechanism of the B–Z junction formation of DNA induced by ZBPs.

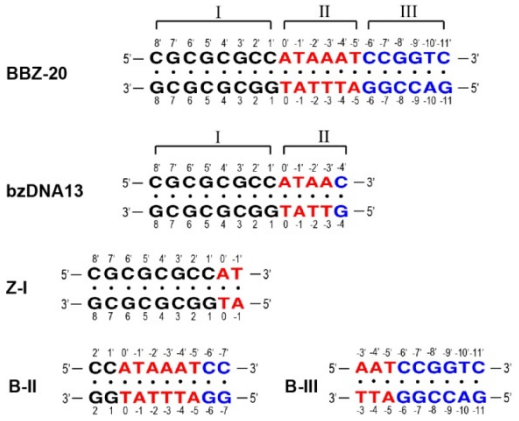

Figure 1. DNA sequence contexts of BBZ-20, bzDNA13, Z-I, B-II, and B-III duplexes.

Experimental Methods

The DNA oligomers were purchased from M-Biotech Inc. (Seoul, Korea) and purified using a Sephadex G-25 gel filtration column. The DNA duplexes were prepared by dissolving two DNA strands at a 1:1 stoichiometric ratio in a 90% H_2O/10% D_2O NMR buffer containing 10 mM sodium phosphate (pH 8.0) and 100 mM NaCl. To produce ^{15}N-labeled $Z\alpha_{ADAR1}$, BL21(DE3) bacteria expressing $Z\alpha_{ADAR1}$ were grown in M9 medium containing 1 g/L $^{15}NH_4Cl$. The expression and purification of ^{15}N-labeled $Z\alpha_{ADAR1}$ have been described in a previous report.[11] The protein concentration was measured spectroscopically using an extinction coefficient of 6970 $M^{-1}cm^{-1}$ at 280 nm.

All NMR experiments were performed on an Agilent DD2 700-MHz spectrophotometer (GNU, Jinju) equipped with cold probe. All NMR data were processed with FELIX2004 software (FELIX NMR, CA, USA). The imino proton resonances in the duplexes are assigned using Watergate-NOESY spectra (mixing times of 120 and 250 ms).

The apparent longitudinal relaxation rate constants of the imino protons ($R_{1a} = 1/T_{1a}$) were determined by semi-selective inversion recovery 1D NMR, where a semi-selective 180° inversion pulse was applied to imino proton region (9 – 15.5 ppm) before the jump-return-echo water suppression pulse. The apparent relaxation rate constant of water (R_{1w}) was determined by selective inversion recovery experiment using a DANTE sequence for selective water inversion.[12-14] The hydrogen exchange rate constants of the imino protons (k_{ex}) were measured by a water magnetization transfer, where a selective 180° pulse for water was applied, followed by a variable delay, and then a 3-9-19 acquisition pulse was used to suppress the water signal.[12] The intensities of each imino proton were measured with 20 different delay times ranging from 5 to 100 ms. The k_{ex} for the imino protons was determined by fitting the data towere determined by fitting the data to Eq. (1):

$$\frac{I(t)}{I_0} = 1 - 2\frac{k_{ex}}{(R_{1w} - R_{1a})}(e^{-R_{1a}t} - e^{-R_{1w}t}) \quad (1)$$

where R_{1a} and R_{1w} were the apparent R_1 rates of the imino proton and water, respectively, and I_0 and $I(t)$ are the peak intensities of the imino proton at times zero and t, respectively.[12-15]

Results

The BBZ-20 duplex has an 8-bp CG-repeat segment in region I, a 6-bp AT-rich segment in region II, and a 6-bp CG-rich but non-CG-repeat segment in region III (Fig. 1A). The BBZ-20 has basically the same sequence with that of the previous X-ray study,[8] but one A·T base-pair is added in region II and four base-pairs are added in region III to stabilize the non-CG-repeat region II and III. 2D NOESY spectra were used to assign the imino resonances of the BBZ-20 duplex.

Fig. 2A shows the doublet signals for the A158

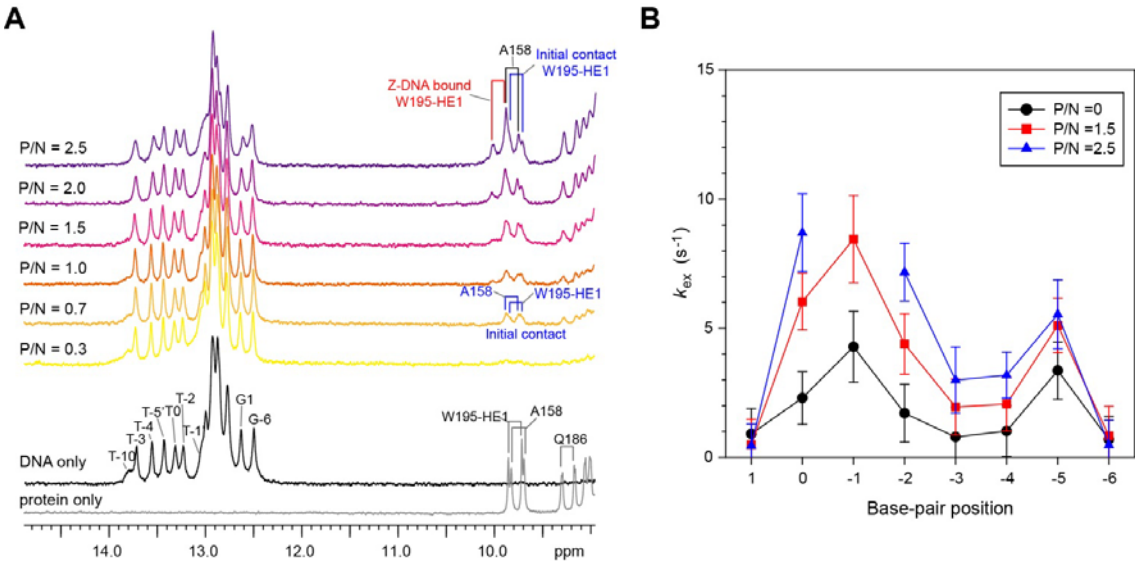

Figure 2. (A) 1D imino spectra of free BBZ-20 and BBZ-20–$Z\alpha_{ADAR1}$ complexes and the same region of 1D spectrum of free ^{15}N-labeled $Z\alpha_{ADAR1}$. (B) The k_{ex} of the imino protons of free BBZ-20 (black circle) and the BBZ-20–$Z\alpha_{ADAR1}$ complexes (P/N=1.5, red square; 2.5, blue triangle) at 35 °C.

amide proton and W195-Hε1 side-chain of the ^{15}N-labeled $Z\alpha_{ADAR1}$ in the complex with BBZ-20, which are caused by ^{15}N-^{1}H heteronuclear *J* coupling (J_{NH} = 93 Hz). The previous study reported that the chemical shift of W195-Hε1 side-chain in the $Z\alpha_{ADAR1}$–bzDNA13 complex displays the initial contact conformation at P/N ≤ 1.0 but shows Z-DNA bound conformation at P/N = 2.0.[9] Similarly, we observed the severely broadened W195-Hε1 signal displaying the initial contact conformation at P/N ratio = 0.7 (Fig. 2A). At P/N = 2.5, the $Z\alpha_{ADAR1}$–BBZ-20 complex exhibits two W195-Hε1 signals; one comes from the initial conformation, and the other from the Z-DNA bound conformation (Fig. 2A). These results suggested that (*i*) when P/N ≤ 1, the $Z\alpha_{ADAR1}$ exhibits an initial contact conformation in which the protein interacts with BBZ-20 and (*ii*) when P/N > 1, $Z\alpha_{ADAR1}$ exhibits properties of both conformations.

Fig. 2A also shows the 1D imino spectra of the BBZ-20−$Z\alpha_{ADAR1}$ complexes. As the P/N is increased, the peak intensity for the T−10' proton significantly decreased until it completely disappeared at P/N = 2.0 (Fig. 2A). The previous study found that in the 13-bp bzDNA13, the T−2 and T−3 imino resonances completely disappeared at P/N = 0.9.[9] However, $Z\alpha_{ADAR1}$ binding did not change the peak intensities in the BBZ-20 when P/N ≤ 2.5 (Fig. 2A).

In order to more clearly probe the effect of $Z\alpha_{ADAR1}$ binding in the BBZ-20, the k_{ex} of the imino protons in free BBZ-20 and BBZ-20−$Z\alpha_{ADAR1}$ complexes at two P/N ratios was determined at 35 °C. We could determine the k_{ex} values of the well-resolved T imino protons in the AT-rich part II and two G imino protons (G1 and G−6), whereas the k_{ex} of other G imino protons were not determined because of their resonance overlaps (Fig. 2A).

The T imino protons in BBZ-20 have k_{ex} from 0.8 to 4.3 s^{-1} at 35 °C. In the 13-bp bzDNA13, the T–3 and T–2 imino protons have the k_{ex} of 54.4 and 13.9 s^{-1}, respectively, whereas other T imino protons have k_{ex} < 6 s^{-1}.[9] These mean that the A·T base-pairs in part II of BBZ-20 are significantly stabilized by the structurally expanded CG-rich region III compared to the 13-bp bzDNA13.

In the BBZ-20−$Z\alpha_{ADAR1}$ complex (P/N =1.5), the T0 imino proton has the k_{ex} of 6.0 s^{-1}, that is 3-times larger than that of free BBZ-20 (Fig. 2B). As the P/N is increased up to 2.5, the k_{ex} of the T0 imino became 8.7 s^{-1} (Fig. 2B). Similarly, the T–1', T–2, T–3, T–4,

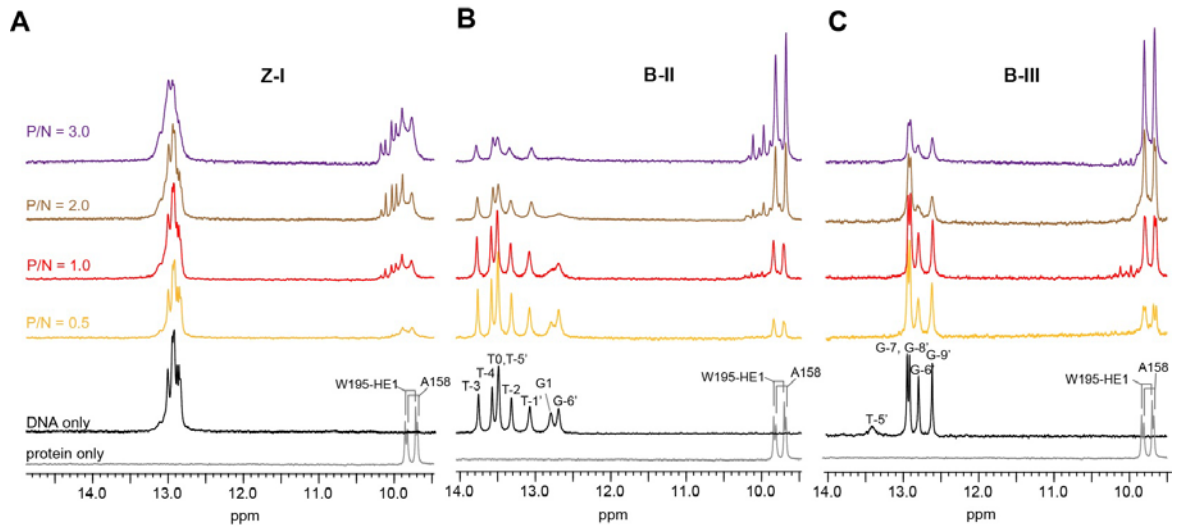

Figure 3. 1D imino spectra of (A) Z-I–$Z\alpha_{ADAR1}$, (B) B-II–$Z\alpha_{ADAR1}$, and (C) B-III–$Z\alpha_{ADAR1}$ complexes at various P/N ratio. The same region of 1D spectra of free DNA and free ^{15}N-labeled $Z\alpha_{ADAR1}$ is shown to the bottom of each spectrum.

and T–5' imino protons have 2- – 2.5-fold larger k_{ex} in the complex (P/N = 1.5) compared to free DNA (Fig. 2B). In the case of bzDNA13 (P/N =0.7), the T0 and T–1' imino protons in the complex with $Z\alpha_{ADAR1}$ have much larger k_{ex} than free form.[9] However, the T–2 imino proton in the complex are 10-fold larger k_{ex} than free bzDNA13.[9] In addition, the T–3 imino resonance disappeared in the complex with $Z\alpha_{ADAR1}$.[9] These results indicate that the binding of $Z\alpha_{ADAR1}$ to the CG-repeat part significantly can destabilize at least 6 base-pairs of neighboring AT-rich segment in a DNA duplex. In the bzDNA13−$Z\alpha_{ADAR1}$, the extreme destabilization of the T–2·A–2' and T–3·A–3' pairs might be contributed by both the binding of $Z\alpha_{ADAR1}$ and the instability of terminal region of DNA duplex.

It is still unclear that the destabilization of the AT-rich part II is caused by structural change induced by binding of the CG-repeat part I with $Z\alpha_{ADAR1}$ or direct interaction with proteins. In order to answer this question, we carried out NMR experiments on the three DNA duplexes, which are designed from cutting the BBZ-20 duplex; the Z-I contains the region I and two base-pairs of region II; the B-II has the region II and two flanking base-pairs at each terminal; the B-III consists of the region III and three base-pairs of region II (Fig. 1). Fig. 3 shows the 1D imino spectra of the Z-I, B-II, and B-III complexed with $Z\alpha_{ADAR1}$ at various P/N ratios. The $Z\alpha_{ADAR1}$ caused a slight line-broadening for the imino resonances of Z-I, without including any changes in their peak intensities (Fig. 3A). The change of A158 amide and W195-Hε1 side-chain resonances indicates the B-Z transition of the CG-rich Z-I duplex (Fig. 3A).

In the B-II and B-III DNA in the complexes with $Z\alpha_{ADAR1}$, the intensities of all imino peaks significantly decreased, as the P/N is increased (Fig. 3B and 3C). Interestingly, the A158-NH and W195-Hε1 signals of the B-II–$Z\alpha_{ADAR1}$ and B-III–$Z\alpha_{ADAR1}$ complexes had the same chemical shifts as those of free $Z\alpha_{ADAR1}$ (Fig. 3B and 3C). This means that B-II and B-III are not converted to Z-DNA, even though the imino resonances are changed by the interaction with protein.

Next, we performed the competition assay using NMR to clarify which DNA duplex first binds to $Z\alpha_{ADAR1}$ among Z-I, B-II, and B-III. Fig. 4A shows changes in the 1D imino spectra of the mixture of Z-I and B-III upon binding to $Z\alpha_{ADAR1}$. Even though the

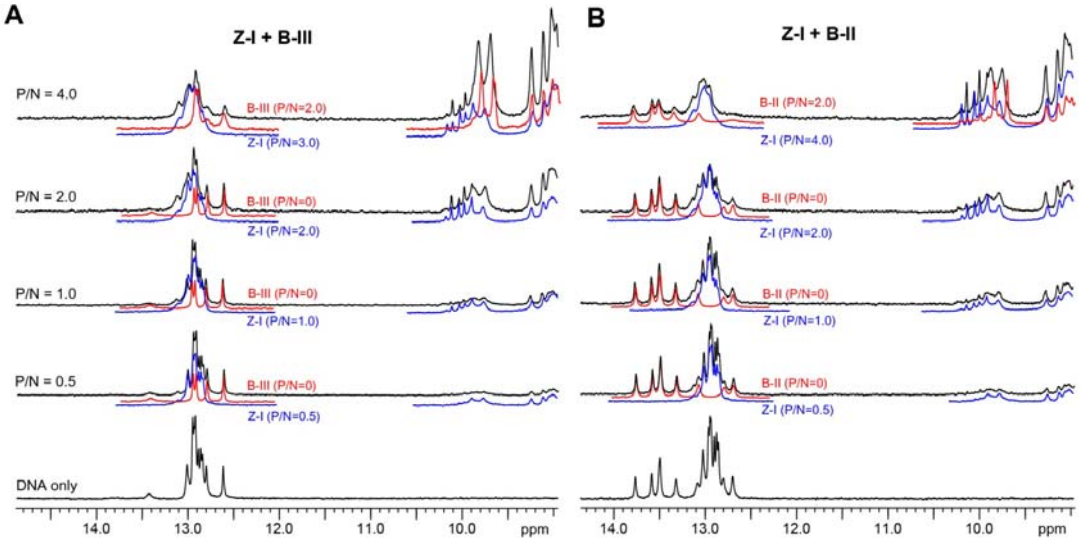

Figure 4. 1D imino spectra of titration of $Z\alpha_{ADAR1}$ to the (A) Z-I and B-III mixture and (B) Z-I and B-II mixture. The same region of 1D spectra of free DNA is shown to the bottom of each spectrum. The blue spectra indicate the 1D imino spectra of the Z-I–$Z\alpha_{ADAR1}$ complex at specific P/N ratio. The red spectra indicate the 1D imino spectra of the B-III–$Z\alpha_{ADAR1}$ (in A) and B-II–$Z\alpha_{ADAR1}$ complexes (in B) at specific P/N ratio.

P/N became 2, the G–6 and G–9' resonances of B-III are the same with those of free B-III (red spectra in Fig. 4A). Instead, the changes of the imino spectra represented the complex formation of Z-I with $Z\alpha_{ADAR1}$ at specific P/N ratio (blue spectra in Fig. 4A). These results indicate that that $Z\alpha_{ADAR1}$ prefer to bind to the CG-repeat Z-I DNA rather than non-CG-repeat CG-rich B-III DNA.

Fig. 4B shows changes in the 1D imino NMR spectra of the mixture of Z-I and B-II upon binding to $Z\alpha_{ADAR1}$. Similar to B-III, all resonances of B-II are the same with those of free B-II (red spectra in Fig. 4B), although the P/N became 2. The imino resonance cluster near 13 ppm in these spectra is well matched the corresponding imino proton spectra of the Z-I duplex with $Z\alpha_{ADAR1}$ at specific P/N ratio (blue spectra in Fig. 4B). These results indicate that that $Z\alpha_{ADAR1}$ prefer to bind to the CG-repeat Z-I DNA rather than AT-rich B-II DNA.

In summary, our NMR study revealed that $Z\alpha_{ADAR1}$ preferentially binds to the CG-repeat segment in a long DNA rather than non-CG-repeat region and then destabilizes at least 6 base-pairs in the neighboring AT-rich sequence for efficient B–Z transition of the CG-rich region.

Acknowledgements

This work was supported by the National Research Foundation of Korea (NRF) Grants funded by the Korean Government (MSIP) [2017R1A2B2001832]. This work was also supported by a grant from Next-Generation BioGreen 21 Program (SSAC, no. PJ01117701). We thank the GNU Central Instrument Facility for performing the NMR experiments.

References

1. A. Herbert, and A. Rich, *J. Biol. Chem.*, **271**, 11595 (1996)
2. A. Herbert, and A. Rich, *Genetica*, **106**, 37 (1999)
3. A. Rich, and S. Zhang, *Nat. Rev. Genet.*, **4**, 566, (2003)
4. T. Schwartz, M. A. Rould, K. Lowenhapt, A. Herbert, and A. Rich, *Science*, **284**, 1841 (1999)
5. T. Schwartz, J. Behlke, K. Lowenhapt, U. Heinemann, and A. Rich, *Nat. Struct. Biol*., **8**, 761 (2001)
6. S. C. Ha, N. K. Lokanath, D. Van Quyen, C. A. Wu, K. Lowenhapt, A. Rich, Y. G. Kim, and K. K. Kim, *Proc. Natl. Acad. Sci. USA*, **101**, 14367 (2004)
7. D. Kim, J. Hur, K. Park, S. Bae, D. Shin, S. C. Ha, H. Y. Hwang, S. Hohng, J.-H. Lee, S. Lee, Y. G. Kim, and K. K. Kim, *Nucleic Acids Res.*, **42**, 5937 (2014)
8. S. C. Ha, K. Lowenhaupt, A. Rich, Y.-G. Kim, and K. K. Kim, *Nature*, **437**, 1183 (2005)
9. Y.-M. Lee, H.-E. Kim, C.-J. Park, A.-R. Lee, H.-C. Ahn, S. J. Cho, K.-H. Choi, B.-S. Choi, and J.-H. Lee, *J. Am. Chem. Soc.*, **134**, 5276 (2012)
10. Y.-M. Lee, H.-E. Kim, E.-H. Lee, Y.-J. Seo, A.-R. Lee, and J.-H. Lee, *Biophys Chem.*, **172**, 18 (2013)
11. Y.-M. Kang, J. Bnag, E.-H. Lee, H.-C. Ahn, Y.-J. Seo, K. K. Kim, Y.-G. Kim, B.-S. Choi, and J.-H. Lee, *J. Am. Chem. Soc.*, **131**, 11485 (2009)
12. J-.H. Lee, and A. Pardi, *Nucleic Acids Res.*, **35**, 2965 (2007)
13. Y.-J. Seo, H.-C. Ahn, E.-H. Lee, J. Bang, Y.-M. Kang, H.-E. Kim, Y.-M. Lee, K. Kim, B.-S. Choi, and J.-H. Lee, *FEBS Lett.*, **584**, 4344 (2010)
14. H.-E. Kim, Y.-G. Choi, A.-R. Lee, Y.-J. Seo, M.-Y. Kwon, and J.-H. Lee, *J. Kor. Magn. Reson. Soc.*, **18**, 52 (2014)
15. Y.-G. Choi, H.-E. Kim, and J.-H. Lee, *J. Kor. Magn. Reson. Soc.*, **17**, 76 (2013)